

Enhancement of the Doppler-free saturated absorption signal based on ^{87}Rb second excited state transition at 420 nm

Yuechen Zhang(张悦晨), Weihao Zhao(赵伟昊), Yuan Tian(田原), Yi Zhang(张奕), Sihong Gu(顾思洪), Ang Zhang(张昂), Jiehua Chen(陈杰华)

Citation: Chin. Phys. B. 35, 094209 (2026). DOI: 10.1088/1674-1056/ae194c |
CSTR: 32038.14.CPB.ae194c
http://cpb.iphy.ac.cn; http://iopscience.iop.org/cpb

What follows is a list of articles you may be interested in

Decoupling of temporal/spatial broadening effects in Doppler wind LiDAR by 2D spectral analysis

Zhen Liu(刘珍), Yun-Peng Zhang(张云鹏), Xiao-Peng Zhu(竹孝鹏), Ji-Qiao Liu(刘继桥), De-Cang Bi(毕德仓), Wei-Biao Chen(陈卫标)

Chin. Phys. B. 33, 034214 (2024). DOI: 10.1088/1674-1056/ad10fd

Theoretical analysis of the optical rotational Doppler effect under atmospheric turbulence by mode decomposition

Sheng-Jie Ma(马圣杰), Shi-Long Xu(徐世龙), Xiao Dong(董骁), Xin-Yuan Zhang(张鑫源), You-Long Chen(陈友龙), Yi-Hua Hu(胡以华)

Chin. Phys. B. 32, 104208 (2023). DOI: 10.1088/1674-1056/acc1d0

An analytical model for cross-Kerr nonlinearity in a four-level N-type atomic system with Doppler broadening

Dinh Xuan Khoa, Nguyen Huy Bang, Nguyen Le Thuy An, Nguyen Van Phu, Le Van Doai

Chin. Phys. B. 31, 024201 (2022). DOI: 10.1088/1674-1056/ac2d19

Super-sensitivity measurement of tiny Doppler frequency shifts based on parametric amplification and squeezed vacuum state

Zhi-Yuan Wang(王志远), Zi-Jing Zhang(张子静), Yuan Zhao(赵远)

Chin. Phys. B. 30, 074202 (2021). DOI: 10.1088/1674-1056/abe3e5

Dependence of interferogram phase on incident wavenumber and phase stability of Doppler asymmetric spatial heterodyne spectroscopy

Ya-Fei Zhang(张亚飞), Yu-Tao Feng(冯玉涛), Di Fu(傅頔), Peng-Chong Wang(王鹏冲), Jian Sun(孙剑), Qing-Lan Bai(白清兰)

Chin. Phys. B. 29, 104204 (2020). DOI: 10.1088/1674-1056/ab9de8

Enhancement of the Doppler-free saturated absorption signal based on ^{87}Rb second excited state transition at 420 nm

Yuechen Zhang(张悦晨)[1,2], Weihao Zhao(赵伟昊)[1,2], Yuan Tian(田原)[1], Yi Zhang(张奕)[1], Sihong Gu(顾思洪)[1], Ang Zhang(张昂)[3,†], and Jiehua Chen(陈杰华)[1,2,4,5,‡]

[1] *State Key Laboratory of Magnetic Resonance and Atomic and Molecular Physics, Innovation Academy for Precision Measurement Science and Technology, Chinese Academy of Sciences, Wuhan* 430071, *China*
[2] *University of the Chinese Academy of Sciences, Beijing* 100049, *China*
[3] *State Key Laboratory of Power Transmission Equipment Technology, School of Electrical Engineering, Chongqing University, Chongqing* 400044, *China*
[4] *Wuhan Institute of Quantum Technology, Wuhan* 430206, *China*
[5] *GNSS Research Center, Wuhan University, Wuhan* 430079, *China*

(Received 25 July 2025; revised manuscript received 21 October 2025; accepted manuscript online 30 October 2025)

We report on the characterization of Doppler-free resonances detected by probing the $5S_{1/2} \rightarrow 6P_{3/2}$ transition of the ^{87}Rb atom at 420 nm. Compared to the commonly studied 5S→5P transition, the 5S→6P transition offers advantages of higher transition frequency and narrower natural linewidth. We investigate how the pump laser intensity and cell temperature affect the linewidth and amplitude of the saturated absorption signal for the 420-nm second excited state transition $5S_{1/2}$ ($F = 2$) $\rightarrow 6P_{3/2}$ in ^{87}Rb atoms. Furthermore, we introduce a 795-nm repump laser to improve the quality of the saturated absorption signal. At a relatively low vapor cell temperature of 43 °C, the amplitude-to-linewidth ratio increased by 110%. These results are highly relevant for the development of stable ultraviolet laser sources and their associated applications.

Keywords: Doppler-free spectroscopy, repump

PACS: 42.62.Fi, 78.47.nd, 06.30.Ft, 32.70.Jz

DOI: 10.1088/1674-1056/ae194c **CSTR:** 32038.14.CPB.ae194c

1. Introduction

Over the past several decades, advances in laser frequency stabilization techniques have significantly driven progress in precision measurement physics.[1–8] Among these techniques, saturated absorption spectroscopy is one of the most widely used methods for frequency stabilization. This technique offers advantages such as narrow resonance linewidths and simple optical setups. High-resolution spectroscopy based on the 5S→ 6P transition in ^{87}Rb atoms has applications in quantum sensing, quantum information, cold atom physics, and atomic clocks.[9–12]

The $5S_{1/2} \rightarrow 6P_{3/2}$ transition ($\Gamma = 2\pi \times 1.4$ MHz) in Rb atoms features a narrower natural linewidth and a higher transition frequency than the commonly used $5S_{1/2} \rightarrow 5P_{3/}2$ transition ($\Gamma = 2\pi \times 6.06$ MHz), making it highly suitable for precision measurements.[13,14] Pandey's group utilized the $5S_{1/2} \rightarrow 6P_{3/2}$ transition to laser-cool ^{87}Rb atoms, achieving atomic temperatures eight times lower than those obtained using the $5S_{1/2} \rightarrow 5P_{3/2}$ transition.[15] Rosi's group proposed a novel atom interferometry scheme based on the blue 5S→6P transition in ^{87}Rb, demonstrating approximately twice the sensitivity compared to setups based on the conventional 780-nm transition.[16]

In this work, we experimentally investigate the saturated absorption spectroscopy of the $5S_{1/2}$ ($F = 2$)$\rightarrow 6P_{3/2}$ transition in ^{87}Rb atoms.[17] Based on measurements of the linewidth and amplitude of the saturated absorption spectroscopy, we identify the optimal pump laser intensity, probe laser intensity, and vapor cell temperature, providing a reference for the development of highly stable ultraviolet laser sources. To further enhance the signal, we introduced a 795-nm repump laser to drive the $5S_{1/2}$ ($F = 1$) $\rightarrow 5P_{1/2}$ ($F = 2$) transition. This optical pumping process increases the population in the $5S_{1/2}$ ($F = 2$) ground state, and the saturated absorption signal at 420 nm. Our experimental results show that, at a vapor cell temperature of 43 °C, the use of repump laser increases the signal amplitude by 63% and the amplitude-to-linewidth ratio by 110%. Combined with measurements of detection noise, we estimate that short-term frequency stability of 2.7×10^{-13} at 1 s.

2. Experimental setup

Figure 1(a) shows the experimental setup used to investigate the saturated absorption spectroscopy of the $5S_{1/2}$

†Corresponding author. E-mail: zhangang@cqu.edu.cn
‡Corresponding author. E-mail: andychen@apm.ac.cn

© 2026 Chinese Physical Society and IOP Publishing Ltd. All rights, including for text and data mining, AI training, and similar technologies, are reserved.

$(F = 2) \rightarrow 6P_{3/2}$ transition in ^{87}Rb atoms. A 420-nm laser beam, with a linewidth below 300 kHz, is generated by an external cavity diode laser (ECDL). A lens group (LG) and an aperture (A) are used to collimate the beam to a diameter of 2.8 mm. The beam power is adjusted using a half-wave plate ($\lambda/2$) and a polarization beam splitter (PBS). The beam is then reflected by a dichroic mirror (DM), which reflects the 420-nm laser and transmits the 795-nm laser, and is subsequently split into two beams by another PBS. The reflected beam is used as the pump laser and passes through a cylindrical ^{87}Rb vapor cell (30 mm in length and 15 mm in diameter). The transmitted beam serves as the probe laser detected by a photodiode (PD). The cell is enclosed within a dual-layer magnetic shield to minimize interference from external magnetic fields. The cell temperature is maintained with bifilar wire winding driven by AC current.

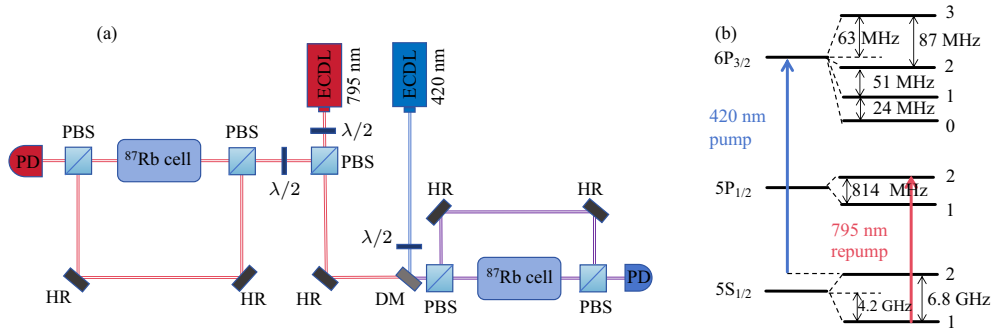


Fig. 1. (a) Experimental setup: $\lambda/2$ half-wave plate, polarization beam splitter (PBS), high-reflection mirror (HR), photodiode (PD), dichroic mirrors (DM); (b) energy level diagram showing the reference transitions at 420 nm and 795 nm of ^{87}Rb.

On the left side of the figure, the saturated absorption setup for the 795-nm transition is shown. This setup, similar to that for the 420-nm transition, is used to lock the laser to the $5S_{1/2}$ $(F = 1) \rightarrow 5P_{1/2}$ $(F = 2)$ transition. The 795-nm beam, with a $1/e^2$ diameter of 3.6 mm, passes through a cylindrical ^{87}Rb vapor cell (30 mm in length and 15 mm in diameter). Once the laser is frequency-locked, the beam is reflected by a mirror and transmitted through the dichroic mirror (DM) to spatially overlap with the 420-nm beam, thereby serving as the repump laser.

3. Experimental results

Firstly, we measure the relative transmission of the probe laser alone under various probe laser intensities. Figure 2 shows the relationship between the relative transmission and the probe laser intensity for the $5S_{1/2}$ $(F = 2) \rightarrow 6P_{3/2}$ transition at a vapor cell temperature of 79 °C. When the probe laser intensity is 0.16 mW/cm^2, the measured transmission is 66%.[18] A significant increase in transmission is observed as the probe intensity approaches 10 mW/cm^2, indicating saturation of the transition due to the strong probe laser field. For the subsequent experiments, we select a probe intensity of 6.5 mW/cm^2 (corresponding to a probe power of 400 μW), as it provides an optimal balance between signal-to-noise ratio and power broadening.

When both the pump and probe laser interact with atoms at zero velocity, a signal without Doppler broadening can be observed. This Doppler-free feature, characterized by a Lorentzian line shape, is detected directly via the counter-propagating probe beam.[19] Figure 3 shows the saturated absorption spectroscopy obtained at 79 °C using probe and pump beams with orthogonal polarizations. The probe power was 400 μW, and the pump power was 4 mW. The x-axis is calibrated using the known frequency separation of 43.5 MHz between the $F = 2 \rightarrow 3'$ and the crossover resonance $F = 2 \rightarrow (2,3)'$.[20] The saturation intensity for the $5S_{1/2} \rightarrow 6P_{3/2}$

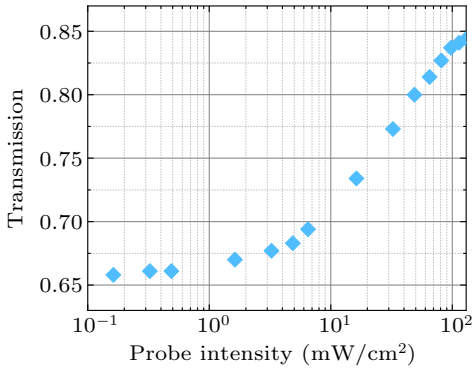


Fig. 2. Relative transmission of the ^{87}Rb $5S_{1/2} \rightarrow 6P_{3/2}$ transition *versus* probe laser intensity, at a vapor cell temperature of 79 °C.

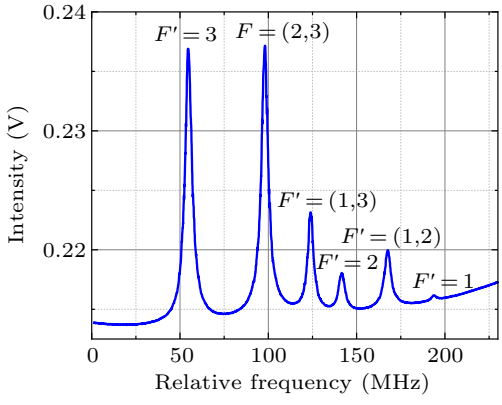


Fig. 3. Saturated absorption spectroscopy of the $5S_{1/2}$ $(F = 2) \rightarrow 6P_{3/2}$ transition, recorded at a vapor cell temperature of 79 °C, with a probe power of 400 μW and a pump power of 4 mW.

transition is calculated to be 2.85 mW/cm^2, using the standard formula $I_{\rm sat} = \frac{\varepsilon_0 c\hbar^2\Gamma^2}{4}|\langle e|d|g\rangle|^2$. Where ε_0 is the vacuum permittivity, c is the speed of light, and $\hbar$ is the reduced Planck constant, Γ denotes the spontaneous decay rate of the excited state, corresponding to 2π times the natural linewidth, $\langle e|d|g\rangle$ represents the electric dipole transition matrix element, where d is the electric dipole operator, and $|g\rangle$ and $|e\rangle$ correspond to the ground and excited states, respectively. The numerical values of the relevant dipole matrix elements are available in the cited references.[21]

An increase in pump laser intensity leads to additional power broadening of the saturated absorption resonances while simultaneously enhancing the amplitude of the saturated absorption signal. The dependence of the linewidth and amplitude for the $5S_{1/2}$ $(F = 2)\rightarrow 6P_{3/2}$ $(F' = 3)$ transition and the crossover resonance $5S_{1/2}$ $(F = 2)\rightarrow$ $6P_{3/2}$ $(F' = 2,\ 3)$ on the pump laser intensity is shown in Fig. 4. As shown in Fig. 4(a), increasing the pump laser intensity shortens the relaxation time of both the ground and excited states, resulting in broader spectral lines.[22] Linewidth broadening due to increasing pump intensity is evident for both resonances. At a pump power of 100 μW, a probe power of 10 μW, and a vapor cell temperature of 79 °C, the measured resonance linewidth of the $5S_{1/2}$ $(F = 2)\rightarrow 6P_{3/2}$ $(F' = 3)$ transition is about 2.5 MHz, which is very close to the natural linewidth ($\sim$ 1.4 MHz).

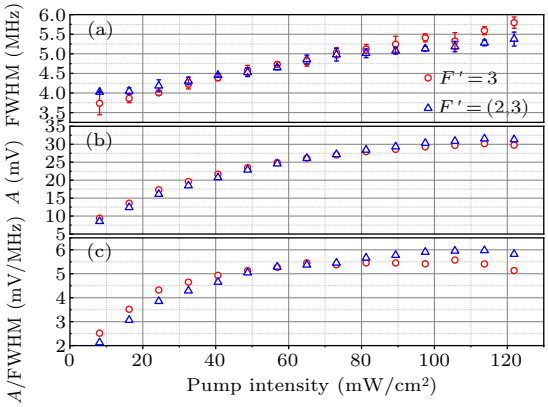


Fig. 4. At a vapor cell temperature of 79 °C and a probe power of 400 μW: (a) full width at half maximum (FWHM) of the saturated absorption resonance for the $5S_{1/2}$ $(F = 2)\rightarrow 6P_{3/2}$ $(F' = 3)$ and the crossover resonance for the $5S_{1/2}$ $(F = 2)\rightarrow 6P_{3/2}$ $(F' = 2,3)$ *versus* pump laser intensity. (b) Amplitude of the saturated absorption signal *versus* pump laser intensity. Error bars represent the standard deviation of four measurements. (c) Amplitude-to-linewidth ratio *versus* pump laser intensity.

Figure 4(b) shows that the amplitude of the saturated absorption signal increases with pump laser intensity, as more atoms participate in the interaction with the laser field. Figure 4(c) presents the dependence of the amplitude-to-linewidth ratio of the saturated absorption signal on the pump laser intensity. For frequency stabilization applications, the pump power density that yields the maximum amplitude-to-linewidth ratio should be selected. According to Fig. 4(c), the optimal pump intensity for the $F' = 3$ resonance is 64 mW/cm^2, corresponding to a pump power of 4 mW. For the crossover resonance $F' = (2,3)$, the optimal pump intensity is 97 mW/cm^2, corresponding to a pump power of 6 mW.

A 420-nm laser continuously acting alone on the atoms can drive a portion of the population into the $5S_{1/2}$ $(F = 1)$ ground state, which does not contribute to the $5S_{1/2}$ $(F = 2)\rightarrow 6P_{3/2}$ resonance. By introducing a 795-nm repump beam resonant with the $5S_{1/2}$ $(F = 1) \rightarrow 5P_{1/2}$ $(F' = 2)$ resonance, atoms can be transferred back to the $5S_{1/2}$ $(F = 2)$ state, hence enhancing the amplitude of the $5S_{1/2}$ $(F = 2)\rightarrow 6P_{3/2}$ $(F' = 3)$ resonance. To investigate this effect, we conducted a detailed study of the enhancement of the 420-nm saturated absorption signal by the 795-nm repump laser. As shown in Fig. 1(a), the frequency-stabilized 795-nm repump beam is combined with the 420-nm laser beam. The repump laser power is fixed at 16 mW.

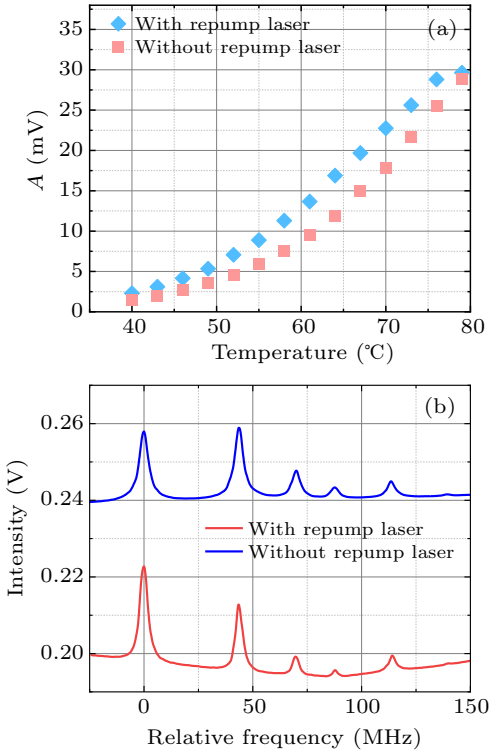


Fig. 5. (a) Dependence of the saturated absorption signal amplitude on vapor cell temperature, with and without the application of repump laser. (b) Saturated absorption spectroscopy recorded at a vapor cell temperature of 70 °C, with and without the application of repump laser.

Figure 5 presents the relationship between the amplitude of the saturated absorption signal for the $F' = 3$ resonance and the vapor cell temperature, both with and without the application of the repump laser. At a vapor cell temperature of 43 °C, the introduction of the repump laser increased the signal amplitude by 63%, while the amplitude-to-linewidth ratio improved by 110%. As the vapor cell temperature increased, the absolute enhancement in signal amplitude induced by the repump laser first increased, then decreased, while the relative improvement gradually diminished. The maximum absolute amplitude enhancement is observed at 70 °C.

Figure 5(b) shows the saturated absorption signals recorded at 70 °C, with and without the repump laser. When

the vapor cell temperature exceeds 79 °C, collisions among atoms and with the cell walls cause atoms in the $5S_{1/2}$ ($F = 1$) ground state to return to the $5S_{1/2}$ ($F = 2$) state, hence reducing the effectiveness of the repump laser in enhancing the signal amplitude. Because the 795-nm repump laser increases the atomic absorption of the pump laser, it weakens the pump laser–atom interaction strength, prolongs the relaxation time of excited-state atoms, and narrows the spectral linewidth. Consequently, the amplitude-to-linewidth ratio improvement reduced to 36% at 79 °C. These experimental results are essential for the subsequent development of compact optical atomic frequency standards.

The short-term frequency stability of a passive atomic frequency reference can be characterized by the expression $\sigma(1\ \mathrm{s}) \approx \frac{1}{Q}\frac{1}{\mathrm{SNR}}$, where the quality factor $Q = \frac{\nu_0}{\Delta\nu}$ is the ratio of the resonance frequency ν_0 to the signal linewidth $\Delta\nu$, and $\mathrm{SNR} = \frac{S}{N}$ is the signal-to-noise ratio. Figure 6 shows the total detection noise at the half-maximum point of the $F' = 3$ saturated absorption signal, recorded at a vapor cell temperature of 79 °C with pump and probe laser powers of 4 mW and 400 μW, respectively. Assuming a modulation frequency of 10 kHz for frequency stabilization, the noise spectroscopy measured using a signal analyzer is −116 $\mathrm{dBV^2/Hz}$, corresponding to a voltage noise of approximately 1.51 μV (with a photodiode gain of 10 dB). The saturated absorption signal has a linewidth of 3.8 MHz and an amplitude of 29.63 mV. Based on these values, the estimated short-term frequency stability is approximately 2.7×10^{-13} at 1 s, which is comparable to other schemes.[23–27]

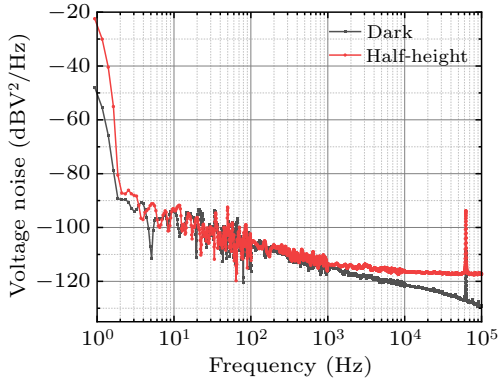


Fig. 6. Detection noise at the photodiode output at the half-maximum point of the $F' = 3$ resonance, with probe laser at 400 μW, pump laser at 4 mW, and vapor cell temperature of 79 °C. The black trace represents the photodiode's dark noise.

4. Conclusion and perspectives

First, we experimentally investigate the saturated absorption spectroscopy of the $5S_{1/2}$ ($F = 2$)→$6P_{3/2}$ ($F' = 3$) transition in ^{87}Rb atoms and determine the optimal values for the pump laser intensity, probe laser intensity, and vapor cell temperature. Furthermore, we demonstrate that applying a frequency-stabilized 795-nm laser on the $5S_{1/2}$ ($F = 1$)→$5P_{1/2}$ ($F' = 2$) resonance as a repump laser significantly enhances the saturated absorption signal of the $5S_{1/2}$ ($F = 2$)→$6P_{3/2}$ ($F' = 3$) resonance. Based on spectral line data and noise measurements, the predicted short-term frequency stability reaches approximately 2.7×10^{-13} at 1 s.

In future work, we aim to develop a compact optical atomic frequency standard based on $5S_{1/2}$ ($F = 2$)→$6P_{3/2}$ ($F' = 3$) transition at 420 nm. The optical system will be designed for simplicity, miniaturization, and operation without the need for modulators.

References

[1] Xiang C, Guo J, Jin W, Wu L, Peters J, Xie W, Chang L, Shen B, Wang H, Yang Q F, Kinghorn D, Paniccia M, Vahala K J, Morton P A and Bowers J E 2021 *Nat. Commun.* **12** 6650
[2] Idjadi M H, Kim K and Fontaine N K 2024 *Nat. Commun* **15** 1922
[3] Lang X, Jia P, Chen Y, Qin L, Liang L, Chen C, Wang Y, Shan X, Ning Y and Wang L 2019 *Sci. China- Inf. Sci.* **62** 61401
[4] Kelleher B, Dillane M and Viktorov E A 2021 *Light Sci. Appl.* **10** 238
[5] DeMille D, Hutzler N R, Rey A M and Zelevinsky T 2024 *Nat. Phys* **20** 741
[6] Chang P, Zhang S, Shang H and Chen J 2019 *Appl. Phys. B* **125** 196
[7] Zhang S N, Zhang X G, Tu J H, Jiang Z J, Shang H S, Zhu C W, Yang W, Cui J Z and Chen J B 2017 *Chin. Phys. Lett.* **34** 74211
[8] Zhang S, Zhang X, Cui J, Jiang Z, Shang H, Zhu C, Chang P, Zhang L, Tu J and Chen J 2017 *Rev. Sci. Instrum.* **88** 103106
[9] Faoro R, Simonelli C, Archimi M, Masella G, Valado M M, Arimondo E, Mannella R, Ciampini D and Morsch O 2016 *Phys. Rev. A* **93** 30701
[10] Degen C L, Reinhard F and Cappellaro P 2017 *Rev. Mod. Phys.* **89** 035002
[11] Monroe C and Kim J 2013 *Science* **339** 1231298
[12] Levine H, Keesling A, Omran A, Bernien H, Schwartz S, Zibrov A S, Endres M, Greiner M, Vuletić V and Lukin M D 2018 *Phys. Rev. Lett.* **121** 123603
[13] Zhang J, Guan X, Gao X, Wang Z, Qin X, Liu Z, Shi H, Miao J, Shi T and Chen J 2024 *Phys. Rev. Appl.* **22** 34045
[14] Vanier J and Audoin C 1989 *The Quantum Physics of Atomic Frequency Standards* (Bristol: Hilger) p. 1258
[15] Das R C, Shylla D, Bera A and Pandey K 2023 *J. Phys. B: At. Mol. Opt. Phys.* **56** 25301
[16] Salvi L, Cacciapuoti L, Tino G M and Rosi G 2023 *Phys. Rev. Lett.* **131** 103401
[17] Zhang A, Zhang Y, Zhao W, Tian Y, Zhang Y, Gu S and Chen J 2024 *Opt. Lett.* **49** 5475
[18] Pizzey D, Briscoe J D, Logue F D, Ponciano-Ojeda F S, Wrathmall S A and Hughes I G 2022 *New J. Phys.* **24** 125001
[19] Smith D A and Hughes I G 2004 *Am. J. Phys.* **72** 631
[20] Das R C, Khan S, Ravi T and Pandey K 2024 *Eur. Phys. J. D* **78** 40
[21] Herold C D, Vaidya V D, Li X, Rolston S L, Porto J V and Safronova M S 2012 *Phys. Rev. Lett.* **109** 243003
[22] Auzinsh M, Budker D and Rochester S 2010 *Optically Polarized Atoms: Understanding Light-atom Interactions* (Oxford, New York: Oxford University Press) p. 169
[23] Klinger E, Mursa A, Rivera-Aguilar C M, Vicarini R, Passilly N and Boudot R 2024 *Opt. Lett.* **49** 1953
[24] Klinger E, Rivera-Aguilar C M, Mursa A, Tanguy Q A A, Passilly N and Boudot R 2025 *Appl. Phys. Lett.* **126** 124003
[25] Newman Z L, Maurice V, Fredrick C, Fortier T, Leopardi H, Hollberg L, Diddams S A, Kitching J and Hummon M T 2021 *Opt. Lett.* **46** 4702
[26] Gusching A, Millo J, Ryger I, Vicarini R, Abdel Hafiz M, Passilly N and Boudot R 2023 *Opt. Lett.* **48** 1526
[27] Newman Z L, Maurice V, Drake T, Stone J R, Briles T C, Spencer D T, Fredrick C, Li Q, Westly D, Ilic B R, Shen B, Suh M G, Yang K Y, Johnson C, Johnson D M S, Hollberg L, Vahala K J, Srinivasan K, Diddams S A, Kitching J, Papp S B and Hummon M T 2019 *Optica* **6** 680